Tribology International 91 (2015) 170–176

Contents lists available at ScienceDirect

Tribology International

journal homepage: www.elsevier.com/locate/triboint

Evaluation of inertia effect in finite hydrodynamic bearings with surface texturing using spectral element solver

Tomasz Woloszynski *, Pawel Podsiadlo, Gwidon W. Stachowiak

Tribology Laboratory, Department of Mechanical Engineering, School of Civil and Mechanical Engineering, Curtin University, GPO Box U1987, Perth, WA 6845, Australia

ARTICLE INFO

Article history:
Received 25 March 2015
Received in revised form
12 June 2015
Accepted 9 July 2015
Available online 17 July 2015

Keywords:
Hydrodynamic
Texturing
Inertia
Spectral element method

ABSTRACT

Fluid inertia can have a major effect on the pressure distribution in hydrodynamic bearings with surface texturing. So far, however, the effect has been ignored in the simulation of finite bearings. In this work, we develop a spectral element solver for the Navier–Stokes equations specifically tailored to slider finite bearings textured with multiple spherical dimples. Using the solver, we studied the effect of inertia on the load-carrying capacity for 90 different bearing configurations. Our results show that the spatial arrangement of dimples has a significant impact on the inertia effect. For the Reynolds number 50 and the ratio 10 of dimple length to dimple depth, a change from full to partial texturing reduced the effect by roughly 85%.

1. Introduction

Hydrodynamic lubrication is an effective way of reducing friction and wear at the contact between two surfaces in relative sliding [1]. One way to form the lubricating film is to texture the surfaces with dimples [2–5]. For certain combinations of the ratio D of dimple length to dimple depth and the Reynolds number Re (roughly $D<50$ for $Re>30$), the lubricant flow transits from purely viscous to visco-inertial [6–8]. This renders the Reynolds equation of viscous lubrication inadequate to simulate the lubricant flow. To rectify this problem, full Navier–Stokes equations (NSE) have been employed instead. However, due to substantial computational effort required to solve the equations in three dimensions (3-D) for complex geometries, studies of the visco-inertial flow in hydrodynamic bearings have been limited to single dimple configurations [8]. In addition, periodic boundary conditions have been used; causing a dependence of results on the location and value of the reference pressure used in solving the NSE [6].

In the current work, we develop a spectral element solver for 3-D NSE that governs the lubricant flow in hydrodynamic bearings with multiple dimples. The solver decomposes the computational domain of the bearing into a small number of pre-defined elements. For each element, a discrete and independent NSE is obtained using the spectral element method (SEM) [9] and a specifically designed Schur complement of the Jacobian matrix. The solution of the NSE for the entire computational domain is obtained by combining the solutions calculated for individual elements, reducing the computational time. Using the solver we conducted a systematic study on the inertia effect in hydrodynamic bearings for 90 different combinations of dimples and the Reynolds numbers, i.e.: 90=15 (spatial arrangements of dimples) × 3 (ratios of dimple length to its depth 10, 50 and 100) × 2 (Reynolds numbers 1 and 50). Other effects such as mass-conserving cavitation and temperature are not studied since they would considerably complicate the numerical simulations. For this reason, a simple Gumbel (half-Sommerfeld) cavitation boundary condition is employed while the effect of temperature on lubricant viscosity is ignored.

2. Methods

For hydrodynamic bearings with laminar and steady flow, and Newtonian, incompressible and isoviscous lubricant, the governing equations consist of the NSE and mass continuity equation

$$\rho\left(u\frac{\partial u}{\partial x}+v\frac{\partial u}{\partial y}+w\frac{\partial u}{\partial z}\right)-\mu\left(\frac{\partial^2 u}{\partial x^2}+\frac{\partial^2 u}{\partial y^2}+\frac{\partial^2 u}{\partial z^2}\right)+\frac{\partial p}{\partial x}=0, \tag{1a}$$

$$\rho\left(u\frac{\partial v}{\partial x}+v\frac{\partial v}{\partial y}+w\frac{\partial v}{\partial z}\right)-\mu\left(\frac{\partial^2 v}{\partial x^2}+\frac{\partial^2 v}{\partial y^2}+\frac{\partial^2 v}{\partial z^2}\right)+\frac{\partial p}{\partial y}=0, \tag{1b}$$

$$\rho\left(u\frac{\partial w}{\partial x}+v\frac{\partial w}{\partial y}+w\frac{\partial w}{\partial z}\right)-\mu\left(\frac{\partial^2 w}{\partial x^2}+\frac{\partial^2 w}{\partial y^2}+\frac{\partial^2 w}{\partial z^2}\right)+\frac{\partial p}{\partial z}=0, \tag{1c}$$

* Corresponding author. Tel.: +61 8 9266 1471.
E-mail address: tomasz.woloszynski@curtin.edu.au (T. Woloszynski).

http://dx.doi.org/10.1016/j.triboint.2015.07.010
0301-679X/

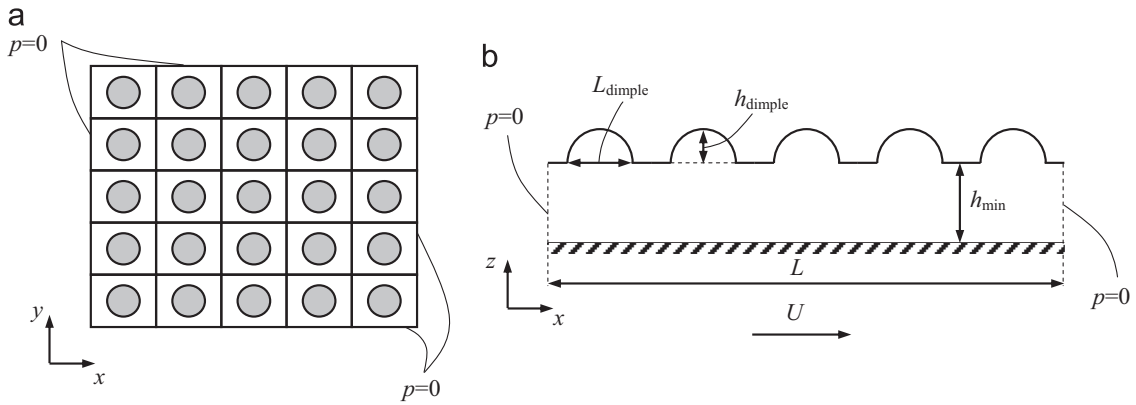

Fig. 1. A schematic diagram of square hydrodynamic slider bearing. (a) Top view showing the grid of 5×5 cells with the top surface of each cell either flat or textured with an elliptical dimple. (b) Side view showing the geometry of dimples. L_{dimple} and h_{dimple} denote the length and depth of a dimple and $h_{\min}$ is the minimum film thickness.

$$\frac{\partial u}{\partial x}+\frac{\partial v}{\partial y}+\frac{\partial w}{\partial z}=0, \tag{1d}$$

where ρ and μ denote the density and dynamic viscosity of the lubricant, p is the pressure function, and u, v and w are the velocity functions in the x, y and z directions, respectively. The unknowns are the pressure and velocity. For the equations to have a unique solution, it is necessary to specify appropriate boundary conditions. In this work, the pressure is set to zero on the boundaries that do not correspond to the bearing surface and the velocity is set to zero (the sliding velocity U) at the boundary that corresponds to the stationary top (sliding bottom) bearing surface (Fig. 1).

In this study, the bearing performance is defined as the load-carrying capacity W^+

$$W^+ = \iint_A p^+ dxdy, \tag{2}$$

where $p^+ = \max(p, 0)$, A denotes the area of the sliding surface and it is assumed that the sliding is in the x direction. The reason for using the load-carrying capacity is that inertial flow mostly affects the pressure distribution [6,7]. The integration is over the positive part of the pressure distribution in Eq. (2) since the Gumbel boundary condition is used in this study.

2.1. Spectral solver

The spectral solver developed in this work first discretises the governing Eqs. (1a)–(1d) into a system of nonlinear algebraic equations using the SEM, and then provides the solution of the system using the Newton's method with preconditioning.

2.1.1. Discretization of the governing equations

Discretization of the governing equations is performed in four steps. First, the governing equations are discretized in a reference domain (i.e., a domain that is independent of the bearing geometry). Next, a physical domain is decomposed into a small number of pre-defined elements. Transformations from the reference domain to each element are then calculated and a system of nonlinear algebraic equations is produced.

2.1.1.1. Discretization in reference domain. 3-D reference domain is defined as a cube $\Omega_* = [-1,1]^3$ with the Cartesian coordinates x_*, y_*, $z_* \in [-1,1]$. For the x_* (y_* and z_*) coordinate, a set of points $x_{*,k}$ $k=1,\ldots,K$ ($y_{*,m}=1,\ldots,M$ and $z_{*,n}=1,\ldots,N$) is chosen based on the nodes of the Gauss–Legendre–Lobatto (GLL) quadrature. Example of the domain for $K=4$, $M=5$ and $N=6$ is shown in Fig. 2. The points are then used to construct a set of Lagrange polynomials $l_{x,k}(x_*)$ ($l_{y,m}(y_*)$ and $l_{z,n}(z_*)$) of degree $K-1$ ($M-1$ and $N-1$) in a such way that the k-th (m-th and n-th) polynomial equals to one at $x_{*,k}$ ($y_{*,m}$ and $z_{*,n}$) and to zero at the remaining points. Using the polynomials, the velocity function in the x direction is approximated as

$$u(x_*, y_*, z_*) \approx \hat{u}(x_*, y_*, z_*) = \sum_{k=1}^{K}\sum_{m=1}^{M}\sum_{n=1}^{N} u_{kmn} l_{kmn}(x_*, y_*, z_*), \tag{3}$$

where u_{kmn} denotes the unknown values to be found and $l_{kmn}(x_*,y_*,z_*)=l_{x,k}(x_*)l_{y,m}(y_*)l_{z,n}(z_*)$. The velocity functions in the y and z directions and the pressure function are approximated similarly. The approximations are then substituted in Eqs. (1a)–(1d) and put into a weak form according to the Galerkin formulation [9]. For first Eq. (1a) the form and the subsequent discretization steps are given by

$$\iiint_{\Omega_*}\left[\rho\left(\hat{u}\frac{\partial \hat{u}}{\partial x_*}+\hat{v}\frac{\partial \hat{u}}{\partial y_*}+\hat{w}\frac{\partial \hat{u}}{\partial z_*}\right)-\mu\left(\frac{\partial^2 \hat{u}}{\partial x_*^2}+\frac{\partial^2 \hat{u}}{\partial y_*^2}+\frac{\partial^2 \hat{u}}{\partial z_*^2}\right)+\frac{\partial \hat{p}}{\partial x_*}\right] l_{rst} d\Omega_* = 0, \tag{4}$$

where $d\Omega_*$ is the volume differential and l_{rst} denotes the same set of polynomials as l_{kmn} except that the indices $r=1,\ldots,K$, $s=1,\ldots,M$ and $t=1,\ldots,N$ are independent of k, m and n. Eq. (4) must be satisfied for all values of the indices r, s and t. Eqs. (1b)–(1d) have similar weak forms. The last step of the discretization in the reference domain is the reduction of the order of derivative in the diffusion term using the divergence theorem

$$\begin{aligned}
&-\iiint_{\Omega_*}\mu\left(\frac{\partial^2 \hat{u}}{\partial x_*^2}+\frac{\partial^2 \hat{u}}{\partial y_*^2}+\frac{\partial^2 \hat{u}}{\partial z_*^2}\right) l_{rst}\ d\Omega_* \\
&=\iiint_{\Omega_*}\mu\left(\frac{\partial \hat{u}}{\partial x_*}\frac{\partial l_{rst}}{\partial x_*}+\frac{\partial \hat{u}}{\partial y_*}\frac{\partial l_{rst}}{\partial y_*}+\frac{\partial \hat{u}}{\partial z_*}\frac{\partial l_{rst}}{\partial z_*}\right) d\Omega_* \\
&-\iint_{S_*}\mu\left(n_{x_*}\frac{\partial \hat{u}}{\partial x_*}+n_{y_*}\frac{\partial \hat{u}}{\partial y_*}+n_{z_*}\frac{\partial \hat{u}}{\partial z_*}\right) l_{rst}\ dS_*,
\end{aligned} \tag{5}$$

where S_* denotes the reference domain boundary, dS_* is the differential element of area and $[n_{x^*}, n_{y^*}, n_{z^*}]$ is the unit normal vector pointing outward from the reference domain. Substituting Eq. (5) into Eq. (4) gives the final form of the discretized Eq. (1a) in the reference domain.

2.1.1.2. Decomposition of physical domain into elements. The physical domain of the bearing is decomposed in two steps. First, the domain is decomposed into a grid of 5×5 cells (Fig. 3a). The cells represent the lubricant volume between the stationary top and sliding bottom bearing surfaces. For each cell, the top surface is either flat or textured with a single spherical dimple and the bottom surface is flat. Second, each cell with textured (flat) top surface is decomposed into five (one) elements (Fig. 3b). The decomposition of the textured cell ensures that the top surface of each element is smooth, increasing the accuracy of spectral approximation [9,10] and the overall number of grid/mesh points is kept as low as possible by means of a trade-off between the